The Journal of Experimental Medicine

Lymph Node Fibroblastic Reticular Cells Construct the Stromal Reticulum via Contact with Lymphocytes

Tomoya Katakai,[1] Takahiro Hara,[1] Manabu Sugai,[1] Hiroyuki Gonda,[1,2] and Akira Shimizu[1,2]

[1]*Center for Molecular Biology and Genetics, Kyoto University and* [2]*Translational Research Center, Kyoto University Hospital, Shogoin-Kawahara-cho, Kyoto 606-8507, Japan*

Abstract

The sophisticated microarchitecture of the lymph node, which is largely supported by a reticular network of fibroblastic reticular cells (FRCs) and extracellular matrix, is essential for immune function. How FRCs form the elaborate network and remodel it in response to lymphocyte activation is not understood. In this work, we established ERTR7$^+$gp38$^+$VCAM-1$^+$ FRC lines and examined the production of the ER-TR7 antigen. Multiple chemokines produced by FRCs induced T cell and dendritic cell chemotaxis and adhesion to the FRC surface. FRCs can secrete the ER-TR7 antigen as an extracellular matrix component to make a reticular meshwork in response to contact with lymphocytes. The formation of the meshwork is induced by stimulation with tumor necrosis factor-α or lymphotoxin-α in combination with agonistic antibody to lymphotoxin-β receptor in a nuclear factor-κB (RelA)–dependent manner. These findings suggest that signals from lymphocytes induce FRCs to form the network that supports the movement and interactions of immune effectors within the lymph node.

Key words: lymphoid tissue • stromal cells • reticular network • ER-TR7 • lymphotoxins

Introduction

Secondary lymphoid tissues, including spleen, LNs, and mucosal-associated lymphoid tissues, function as sites for the maturation, activation, and maintenance of peripheral lymphocytes needed to produce efficient immune responses (1–3). Especially, LNs are strategically located at the downstream neck of lymphatics drained from peripheral tissues, filtrating or monitoring the tissue fluid exudate carrying information about the peripheral tissues. These LN functions are performed via a unique microarchitecture in which distinct subsets of immunohematopoietic cells are strategically compartmentalized (2–6). The localizations of B and T lymphocytes, clearly separated in the cortical region, are most pronounced (see Fig. 1 a). B cells organize follicles (B zone) in the outer cortex and occasionally develop germinal centers (GCs) during T cell–dependent immune responses. A majority of T cells reside in the paracortex (T zone) underneath the follicles extending to the cortico–medullary junction. DCs carrying information about peripheral tissues arrive at the subcapsular sinus (SCS) through afferent lymphatics and further migrate into the T zone to interact with T cells (7). Several macrophage subsets are mainly distributed in the medullary sinus and SCS regions, where they trap and phagocytose large particles (8).

Because lymphocytes are generally nonstatic and mobile, it seems reasonable to predict that stromal populations would support their distribution and locomotion as a structural backbone within the LN. Actually, several cell types of endothelial and mesenchymal origin are responsible for this task (see Fig. 1 a). The blood endothelial cells comprising the vascular network are remarkable. Blood vessels entering the LN branch off extensively at the medullary region, which is thus rich in these vessels, and penetrate throughout the cortex. In the paracortex, endothelial cells form a specialized structure, the high endothelial venule (HEV), which plays important roles in lymphocyte homing or recirculation (6, 9, 10). In contrast, follicular DCs (FDCs) are a stromal population of mesenchymal origin supporting follicles or GCs. They retain antigens for a long period and are involved in B cell attraction, activation, and maturation (5).

Address correspondence to Tomoya Katakai, Center for Molecular Biology and Genetics, Kyoto University, 53 Shogoin-Kawahara-cho, Sakyo-ku, Kyoto 606-8507, Japan. Phone: 81-75-751-4194; Fax: 81-75-751-4190; email: tkatakai@virus.kyoto-u.ac.jp

Abbreviations used in this paper: BLS, BALB/c LN stroma; ECM, extracellular matrix; FDC, follicular dendritic cell; FRC, fibroblastic reticular cell; GC, germinal center; HEV, high endothelial venule; LT, lymphotoxin; LTi, lymphoid tissue inducer; PTx, pertussis toxin; RF, reticular fiber; RN, reticular network; SCS, subcapsular sinus.

 J. Exp. Med. © The Rockefeller University Press • 0022-1007/2004/09/783/13 $8.00
Volume 200, Number 6, September 20, 2004 783–795
http://www.jem.org/cgi/doi/10.1084/jem.20040254

Of prime importance, the whole tissue architecture of the LN (including the aforementioned stromal populations) is entirely supported by the reticular network (RN; see Fig. 1, a and b). This intricate meshlike structure is composed of reticular fibers (RFs), fibrous extracellular matrix (ECM) bundles, and another mesenchymal cell population, fibroblastic reticular cells (FRCs; 6, 11–15). In marked contrast to most of the fibroblasts in connective tissues, which are embedded in the ECM (16), FRCs in the LN ensheath the thin strands of ECM, while they are also continually in contact with immune cells (12). The characteristic network made by FRCs appears to be optimal for simultaneously providing mechanical strength to the tissue and making spaces for motile immune cells to move through. In addition, it may function as a physical barrier for the compartmentalization of immune cells to prohibit their disordered interactions or massive growth. However, what makes the FRCs build this elaborate network is still a mystery. Although FRCs are more plentiful than other stromal populations within the LN, the physiological roles of FRCs in immune responses also remain poorly understood. Recently, Shaw et al. have shed light on a part of FRC/RN function with intriguing concepts such as "paracortical cord" or "conduit," etc. (11–13). The lymphoid stroma is considered to provide the environmental basis for the cytokine and chemokine fields for lymphocyte activation or regulation (17, 18). Precisely identifying the microanatomical sites (including the underlying stromal milieu) where the immune response is in progress will help to advance our understanding of various infections, allograft rejection, autoimmune diseases, and tumor metastasis. Accordingly, characterization of the cellular and molecular nature of the FRC/RN is an important goal at this time.

Based on findings from various gene-targeting mouse models, our knowledge about the molecular basis of the development of secondary lymphoid tissues has greatly advanced in the past decade. A key event is an interaction between $CD3^-CD4^+CD45^+$ hematopoietic "inducer" (lymphoid tissue inducer [LTi]) cells expressing lymphotoxin (LT)-$\alpha1\beta2$ on their surface and VCAM-1^+ICAM-1^+ mesenchymal "organizer" cells expressing LTβR during restricted periods of embryogenesis (19–21). Components of the downstream signaling pathway of LTβR, such as NF-κB–inducing kinase, IκB kinase α, and NF-κB family transcription factors, are also essential for the differentiation of the mesenchymal cells into cells that express a specific set of adhesion molecules and chemokines (19–21). However, the details of stromal responses in the lymphoid tissue anlagen remain largely unclear. Because stromal populations in adult lymphoid tissues are thought to be direct descendants of the organizer cells or their derivatives, the adult-type cells are likely to preserve some features of embryonic organizers. Therefore, to investigate the stromal cells in adult tissue may provide useful information about the process of lymphoid organogenesis as well as the maintenance of tissue architecture thereafter.

Here, we studied in detail the features of FRCs by establishing cell lines from the mouse LNs that could attract and adhere to T cells and DCs, as well as produce an ER-TR7 meshwork in the presence of lymphocytes in vitro. Our findings support the notion that lymphocytes and stromal cells collaboratively construct the specialized supporting milieu and, thus, FRCs actively participate in immune responses within the LN. These insights could be applied to what occurs in the lymphoid tissue anlagen and the later maturation of the stromal network.

Materials and Methods

Mice. BALB/c mice were maintained at the animal care facility in the Center for Molecular Biology and Genetics at Kyoto University. Procedures involving animals and their care were conducted according to the guidelines for animal treatment of the Institute of Laboratory Animals at Kyoto University. Mice were immunized subcutaneously with 100–200 μg OVA in a 1:1 mixture of PBS and alum adjuvant (Inject Alum; Pierce Chemical Co.) or in a 1:1 emulsion of PBS and CFA (Difco) in the footpads.

Antibodies. The antibodies used for immunohistochemistry or flow cytometry were as follows: as primary reagents, ER-TR7 (BMA), biotin anti-CD3, biotin anti-CD4, FITC anti-B220, anti-CR1, FITC anti-CD11c, PE anti-CD44, biotin anti-CD80 (BD Biosciences), anti–PECAM-1 (Caltag), anti–Mac-1, anti–VCAM-1 (Immunotech), antilaminin (LSL; Cosmo Bio), anti-RelA (p65), anti-RelB (Santa Cruz Biotechnology, Inc.), anti-FcγRII/III, anti–MHC class II, anti–ICAM-1, anti-CD44, anti-gp38 (22) (hybridoma supernatants), and biotin anti–BP-3 antibody (23); as secondary reagents, PE anti–rat IgG, FITC anti–hamster IgG, biotin anti–rat IgG (Caltag), FITC anti–rabbit IgG antibody (Jackson ImmunoResearch Laboratories), PE streptavidin, and allophycocyanin-streptavidin (Molecular Probes). Polyclonal goat antibody against LTβR extracellular domain and control IgG for cell stimulation were purchased from R&D Systems.

Cells. FRC cell lines were established from peripheral LNs of BALB/c mice by long-term culturing. After the LN single cell suspension was placed into a tissue culture dish with 10% FCS-DMEM for 24 h, nonadherent cells were removed, fresh medium was added, and culturing was continued for several weeks, during which fibroblast-like adherent cells grew at a very slow rate. After several months of further incubation while exchanging the medium every few weeks, relatively fast-growing cells that formed a colony were harvested and passaged repeatedly to produce the stable cell lines. Macrophages and DCs were eliminated from the culture based on the facts that they grew less or were harder to obtain by trypsinization, and were therefore finally diluted out. Among 12 cell lines established, we chose BALB/c LN stroma (BLS)1, BLS4, BLS6, and BLS12 for further analysis because of their moderate proliferation and the fact that they exhibited contact inhibition. For transfection experiments, cDNAs encoding GFP or Iκ''' BαSR (24) were ligated into pMX-puro retroviral vector (25). Retroviruses were produced by transfection of the constructs into the Phoenix-Eco packaging cell line (26). BLS cells were infected with retroviruses and selected with 5–10 μg/ml puromycin.

LN cells were prepared as a single cell suspension of pooled peripheral LNs from BALB/c mice by removing plastic plate-adherent cells. $CD4^+$ cells were further separated as the bound fraction of magnetic cell sorting (MACS; Miltenyi Biotec) using biotin anti-CD4 antibody (BD Biosciences) followed by streptavidin-MicroBeads (Miltenyi Biotec). DCs were generated from bone marrow as described previously (15, 27, 28).

Immunohistochemistry. 10-μm frozen sections were fixed with cold acetone. FRC lines plated on chamber slides (Nunc) with or

without coculturing or factor treatment were fixed with 3% paraformaldehyde-PBS and permeabilized with 0.2% Triton X-100. Sections or cells stained with antibodies by direct or indirect methods were examined using a confocal laser scanning microscope (MRC-1024; Bio-Rad Laboratories) or a fluorescence microscope (TND330; Nikon) with a 3CCD camera (C5810; Hamamatsu Photonics). Digital images obtained were prepared using Photoshop software (Adobe Systems Inc.). For whole views of the LN, images at different positions were assembled into a single image by combining adjacent images using the same software.

Flow Cytometry. FRC cells were harvested from culture dishes by releasing them with 0.02% EDTA-PBS. The cells were stained with antibodies by direct or indirect methods after blocking with PBS containing 1% BSA and 10% mouse serum. The cells were analyzed using a FACSCalibur flow cytometer with CELLQuest software (Becton Dickinson).

RT-PCR Analysis. Semi-quantitative RT-PCR analysis was performed as described previously with some modifications (29). Specific primer pairs used in this work were as follows: GAPDH, 5′-CCATCACCATCTTCCAGGAG-3′ and 5′-CCTGCTTCACCACCTTCTTG-3′; gp38, 5′-GAATTCCAACGAGATCAAGATGTG-3′ and 5′-GGATCCTTCTTATCTGTTGTCTGCGT-3′; BP-3, 5′-GAGCCTGGGGAACAAAAACT-3′ and 5′-CCCCTGAACTGTCTCTTGAA-3′; CCL4, 5′-CAGCTCTGTGCAAACCTAAC-3′ and 5′-TCAGTTCAACTCCAAGTCAC-3′; CCL5, 5′-TCTGAGACAGCACATGCATC-3′ and 5′-CCTAGCTCATCTCCAAATAG-3′; CCL20, 5′-CCCAGCACTGAGTACATCAA-3′ and 5′-GCATCAGTTTTTTACATCTT-3′; CCL21, 5′-AGCTATGTGCAAACCCTGAG-3′ and 5′-TCATAGGTGCAAGGACAAGG-3′; CXCL10, 5′-AGACATCCCGAGCCAACCTT-3′ and 5′-GTTAAGGAGCCCTTTTAGAC-3′; CX3CL1, 5′-CTTTGCTCATCCGCTATCAG-3′ and 5′-CTCAAAACTTCCAATGCTCT-3′; CCL2, 5′-TCACTGAAGCCAGCTCTCTC-3′ and 5′-CTAGTTCACTGTCACACTGG-3′; CXCL12, 5′-AAACCAGTCAGCCTGAGCTAC-3′ and 5′-TTACTTGTTTAAAGCTTTCTC-3′; and LYVE-1, 5′-CATCTGTCTCCCTTACTGCG-3′ and 5′-TAGGCTTTGAACTTTTGGCT-3′.

Chemotaxis and Adhesion Assays. FRCs with or without stimulation by 10 ng/ml murine TNFα (PeproTech) were cultured in 10-cm culture dishes for 48 h, washed with PBS, and incubated with fresh medium for a further 48 h. Culture supernatants of the FRCs were collected, filtrated, and stored until experiments. Chemotaxis assays using the culture supernatants were performed as described previously (29). For adhesion assays, 5×10^4 CMFDA-labeled, pertussis toxin (PTx)–treated, or -untreated DCs were placed onto BLS monolayers on 24-well cul-

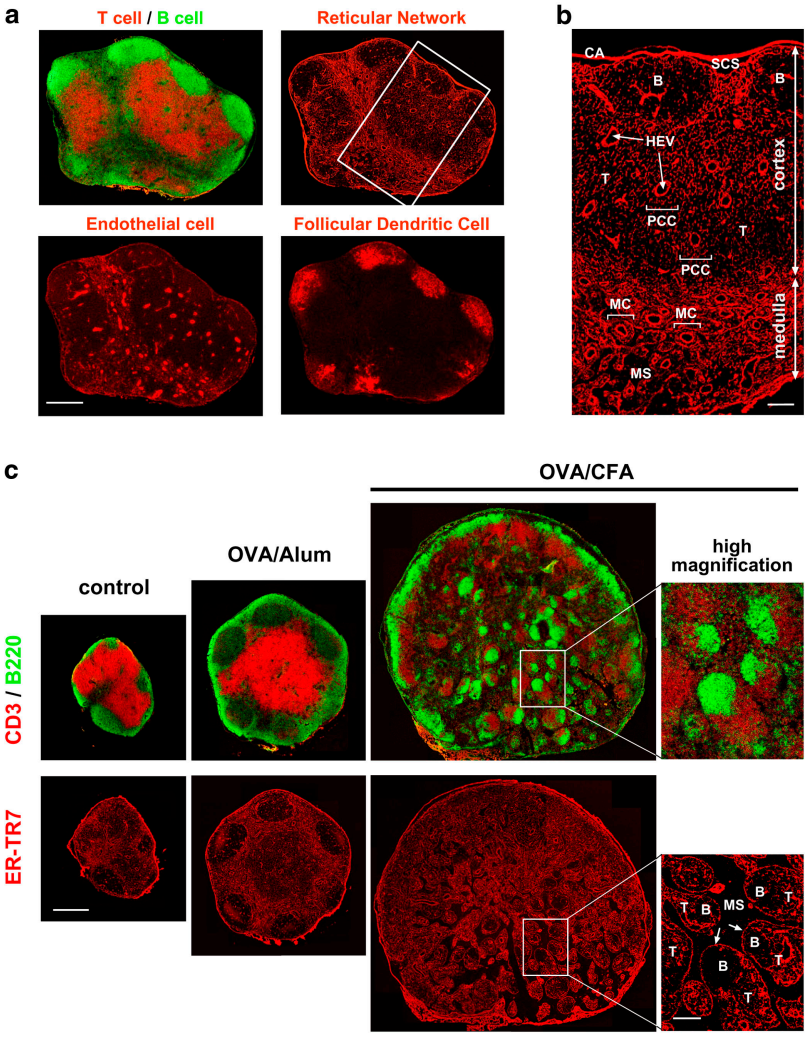

Figure 1. Architecture of the ER-TR7$^+$-RN in mouse LN, and the dynamic remodeling during immune responses. (a) Whole views of LN stromal populations. Serial frozen sections were stained with several antibodies to detect CD3 (T cells), B220 (B cells), ER-TR7 antigen (reticular fibroblasts), PECAM-1 (endothelial cells), or CR1 (FDCs). The images shown are composites of multiple high-magnification images at distinct positions of an LN assembled on silica. Bar, 400 μm. (b) Higher magnification view of RN (inset in panel a) shows subreticular structures or compartments. B, B zone [follicle]; CA, capsule; HEV, high endothelial venule; MC, medullary cord; MS, medullary sinus; PCC, paracortical cord; SCS, subcapsular sinus; T, T zone. Bar, 100 μm. (c) Immunizations with OVA plus adjuvant induce dynamic remodeling of the RN within popliteal LNs. Serial frozen sections of the popliteal LNs from untreated, OVA + alum-, or OVA + CFA-immunized mice were stained with antibodies against CD3, B220, or ER-TR7. Three whole LN images are shown at the same magnification. Higher magnification view of the inset region in the medulla of CFA-immunized LN shows some nodular islands containing discrete B and T zones, enclosed by a single FRC layer (arrows). Bars: 500 μm for whole views and 100 μm for high-magnification views.

ture plates and incubated for 1 h at 37°C (29). After the unbound cells were removed by washing once with PBS, bound DCs and BLS cells were trypsinized to prepare a single cell suspension and analyzed using a FACSCalibur flow cytometer with a constant time period (60 s), counting the DCs as labeled cells.

ER-TR7 Meshwork Formation. Confluent FRC lines grown on chamber slides were cocultured with 10^6 LN cells, $CD4^+$ T cells, or various lymphoid cell lines such as EL4, BW5147, A20.2j, and WEHI231 for various periods up to 10 d. Alternatively, FRCs were stimulated with cytokines or reagents such as 10–100 ng/ml TNFα, 10 ng/ml LTα (human), 10 ng/ml IL-1β, 10 ng/ml IL-4, 5 ng/ml IFNγ, 10 ng/ml TGFβ (PeproTech), 10 μg/ml LPS (Sigma-Aldrich), or 1 μg/ml anti-LTβR antibody (R&D Systems). Subsequently, the same amounts of fresh reagents were again added on d3 and d6. After the culture, cells were fixed and stained with ER-TR7 antibody for assessing the meshwork formation. Quantification of the ER-TR7 meshwork formation was performed using a density slice program of the public domain Image software (developed at U.S. National Institutes of Health and available at http://rsb.info.nih.gov/nih-image). Total pixels (each pixel was represented by a value ranging from 0–255) at high (0–50), medium (51–100), or low (101–150) density windows on an image were measured using the software.

For semi–three-dimensional cultures, FRC lines were grown on autoclaved nylon-mesh (50 μm; Yamamoto) coated with laminin (10 μg/ml in PBS; GIBCO BRL) for 5–7 d, and cocultured with 3×10^6 LN cells in 24-well plates for 8–10 d. Images were obtained using a TCS-SP2 confocal microscope and software system (Leica). Z-stacks (optical sections) of the images were collected and prepared for three-dimensional reconstitution using the software.

Results

Architecture and Dynamic Remodeling of ER-TR7$^+$ RN in the LN. To obtain whole views of LN stromal microarchitecture with high resolution, first we performed fluorescence immunohistochemistry coupled with confocal imag-

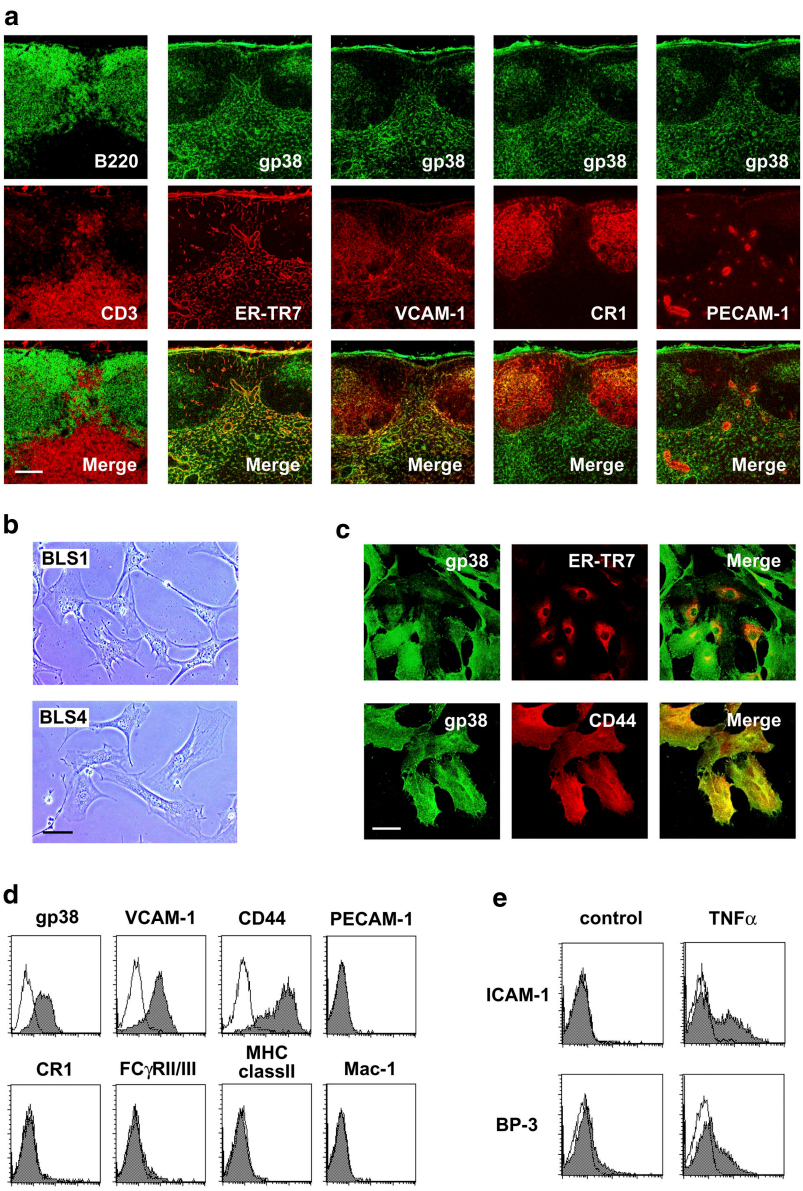

Figure 2. Phenotypic features of FRCs and the establishment of BLS lines. (a) FRCs in the LN are ER-TR7$^+$gp38$^+$VCAM-1$^+$ cells. Serial frozen sections were stained for various markers. Bar, 100 μm. (b) Typical fibroblastic morphology of BLS1 and BLS4 cells. Phase-contrast views of growing cells on plastic dishes are shown. Bar, 50 μm. (c) Intracellular localization of ER-TR7 compared to surface expression of gp38 and CD44 in BLS4 cells. Cells grown on chamber slides were stained with antibodies after fixation and permeabilization. Bar, 50 μm. (d) Cell surface expression of gp38, VCAM-1, and CD44 in BLS4 cells. EDTA-harvested cells were stained for the indicated surface markers and analyzed by flow cytometry. (e) Expression of ICAM-1 and BP-3 is induced by TNFα. Cells were stimulated with TNFα and subsequently stained with anti–ICAM-1 or anti–BP-3 antibody for flow cytometry.

ing. Antibodies against ER-TR7 antigen, PECAM-1, and CR1 are quite useful for detecting LN stromal populations, including FRC, vascular endothelial cells, and FDCs, respectively (Fig. 1 a). Examining the images thus obtained, we were able to observe these kinds of cells distributed in and organizing distinct compartments in the LN. In particular, the FRC/RN structure was clearly visualized using monoclonal antibody ER-TR7, which recognizes a yet-undetermined antigen (30). The RN extended widely in the LN, but local staining of subcompartments such as SCS, follicles, paracortex, and medulla was remarkably diverse (Fig. 1 b and references 12, 15). The close correlation between the RN subregions and the location of immune cell subsets implies that the interaction of FRCs with a certain immune cell subset appears to be required for maintaining the local reticular structure.

For visualizing the changes of the RN during immune responses, we examined popliteal LNs from immunized mice that had been injected with OVA plus adjuvants into the footpad. Under normal conditions, popliteal LNs are relatively small (1≈1.5 mm); however, the immunization enlarged them, with changes in the lymphocyte distributions that were precisely mirrored by changes in the RN compartments (Fig. 1 c). Alum adjuvant, which effectively enhances antigen-specific antibody production, induced moderate tissue swelling with large GCs. The enlargement of popliteal LNs was far more dramatic in mice immunized with CFA; however, the organization of not only lymphocytes but also RN structures was disturbed. Interestingly, small nodular islands appeared in the expanded medulla, in which T and B cells were clearly separated and enclosed by a single layer of FRCs. These findings indicate the extreme plasticity of the RN that FRCs construct and remodel as needed, with the need being determined by sensing immune cells and their activation. Furthermore, because the dynamics of ER-TR7 antigen in the LN are considered to reflect the activity and actions of FRCs, examining these dynamics would provide a valuable index of FRC behavior.

Like ER-TR7, the transmembrane glycoprotein gp38 is a marker for LN FRCs (Fig. 2 a and references 22, 31). Double staining for ER-TR7 and gp38 clearly revealed colocalization of the two markers in the LN sections. We also found that VCAM-1 is an additional marker for FRCs (Fig. 2 a). In contrast, markers specific for FDCs or endothelial cells, CR1 or PECAM-1, respectively, showed patterns almost inverse to those of the FRC markers. Therefore, we considered ER-TR7$^+$gp38$^+$VCAM-1$^+$ cells to be FRCs.

Establishment of FRC Lines from LNs. Studies of FRC/RN have been hampered by the difficulty of isolating a substantial amount of the cells from lymphoid tissues. Therefore, we tried to establish FRC lines from LN adherent cells by long-term culturing (see Materials and Methods), and thereby obtained 12 lines from seven different mice and named these lines the BLS series. All of the BLS lines showed typical fibroblastic morphology and expressed gp38, VCAM-,1 and CD44 on the surface, but did not express detectable PECAM-1, FCγRII/III, CR1, MHC class II, or Mac-1 (Fig. 2, b–d), indicating that they are distinct from endothelial cells, FDCs, and macrophages. Consistent with the initial paper by van Vliet et al. (30), when the cells

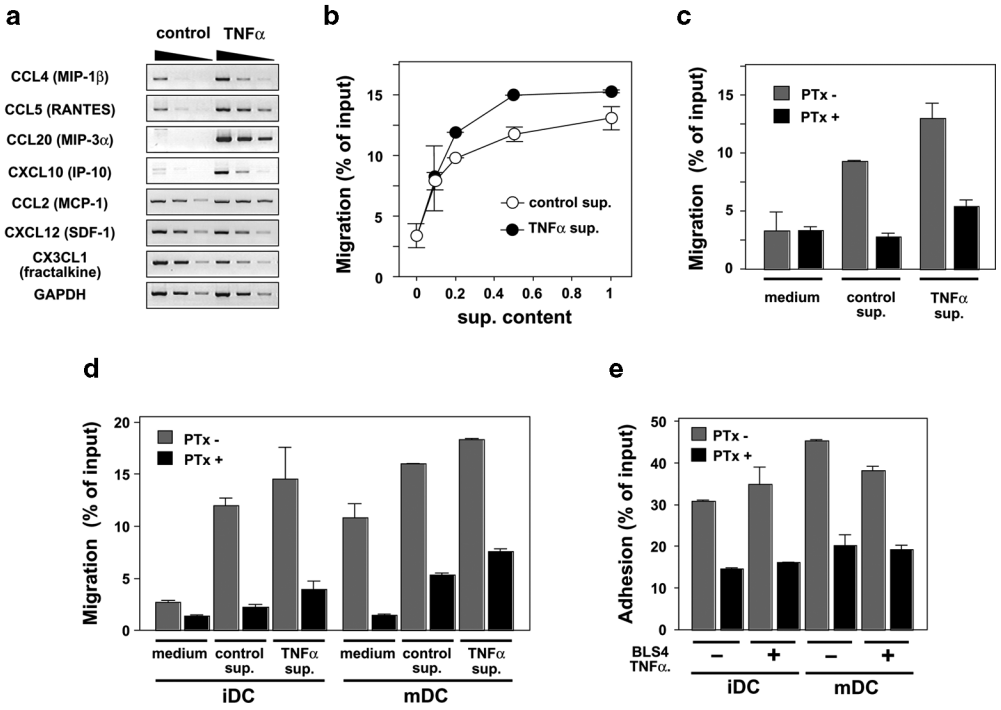

Figure 3. BLS cells support the migration and adhesion of T cells and DCs. (a) BLS4 cells express various chemokines with or without TNFα stimulus. Transcripts for the indicated chemokines were detected by semi-quantitative RT-PCR analysis. (b) BLS4 supernatant (sup.) induces the chemotaxis of CD4$^+$ T cells. The chemotactic activity in diluted culture supernatants from BLS4 cells (prestimulated or not prestimulated with TNFα) was analyzed by a chemotaxis assay. (c) Chemotaxis of CD4$^+$ T cells to the BLS supernatants is Gαi dependent. T cells were pretreated or not pretreated with PTx and subjected to the chemotaxis assay. Two-fold diluted supernatants were used as attractant. (d) BLS4 supernatant induces DC chemotaxis. Immature (iDC) or mature (mDC) DCs were pretreated or not pretreated with PTx and subjected to the chemotaxis assay. (e) BLS4 cells support DC adhesion to their surface. DCs were pretreated or not pretreated with PTx and subjected to the adhesion assay.

were fixed and permeabilized, intracellular ER-TR7 was detected, particularly in the Golgi apparatus and endoplasmic reticulum (Fig. 2 c). In most of the lines, ICAM-1 expression was induced by TNFα stimulation (Fig. 2 e), although some lines expressing ICAM-1 constitutively were also established (not depicted). When BLS4 cells were stimulated with TNFα, we were able to detect weak expression of another lymphoid stromal marker, BP-3 (23), by flow cytometry (Fig. 2 e) and RT-PCR (not depicted). Because BLS cells were negative for a lymphatic vessel marker, LYVE-1 (32), they are different from lymphatic endothelial cells (unpublished data). Based on these findings, we concluded that BLS cells retain the character of FRCs and are suitable for in vitro studies.

FRCs Support the Chemotaxis and Adhesion of T Cells and DCs. The RN may work as the physical base for immune reactions in vivo and, thus, FRCs might directly contribute to the attraction or adhesion of immune cells. BLS cells constantly expressed chemokines such as CCL2, CXCL12, and CX3CL1, whereas the level of expression of CCL4, CCL5, CCL20, and CXCL10 was low in the steady state, but was elevated in response to TNFα (Fig. 3 a). Culture supernatant of BLS4 cells induced chemotaxis of LN $CD4^+$ T cells in a dose-dependent manner, and the stimulation of BLS4 cells with TNFα augmented the level of chemotactic activity in the culture supernatant (Fig. 3 b). Pretreatment of T cells with pertussis toxin (PTx) markedly blocked the chemotaxis (Fig. 3 c), demonstrating the dependence on Gαi-coupled chemokine receptor signal. Resting T cells prepared from LNs generally adhered to BLS cells weakly, whereas T cell lines or cloned T cells exhibited strong adhesion (unpublished data), suggesting that the activation status of T cells regulates the ability to bind to FRCs. BLS supernatants attracted immature DCs in a PTx-sensitive manner (Fig. 3 d), although mature DCs showed some nonspecific migration to the medium and, therefore, the specificity of the effect of BLS-derived chemokines is questionable in this case. BLS cells also supported firm adhesion of DCs onto their surface in a manner partially dependent on chemokines (Fig. 3 e). These findings support the idea that FRCs have the ability to provide guidance cues as well as a foothold for immune cells via chemokines and adhesion molecules.

FRCs Construct ER-TR7 Meshwork. FRCs in the LN appear to continually be in contact with lymphocytes. Because this continuous interaction is thought to be important for the RN formation, we cocultured the monolayers of BLS cells expressing green fluorescent protein with LN cells for >1 wk. Surprisingly, in this coculture system, ER-TR7 did not show an intracellular pattern, but instead was seen as a clear filamentous, interconnected meshwork with some brighter signals (Fig. 4 a). The meshwork was detected without cell permeabilization, indicating that it is located outside the BLS cell body (unpublished data). Of note, ER-TR7 fibers were frequently located at the cell periphery, suggesting that some aspect of plasma membrane dynamism (e.g., actin cytoskeleton-mediated pseudopodial action) in BLS cells might affect the extracellular meshwork assembly (Fig. 4 a, arrowheads). The meshwork also appeared in cocultures with purified $CD4^+$ T cells (Fig. 4 a), T lymphoma cells (such as EL4 or BW5147), and B lymphoma cells (such as A20.2j or WEHI231; not depicted). BLS cells constructed the meshwork gradually as the coculturing proceeded (Fig. 4 b). It was possible to quantify the ER-TR7 meshwork by measuring the pixels with defined

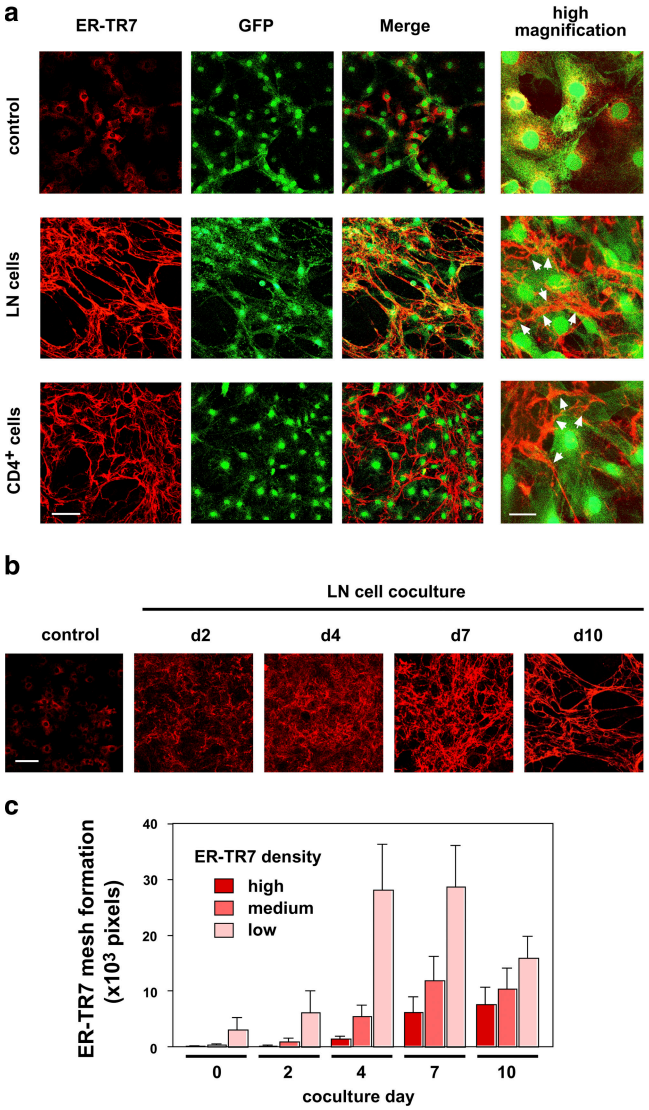

Figure 4. BLS cells construct the ER-TR7 meshwork via contact with lymphocytes. (a) ER-TR7 meshwork formation by BLS4 cells cocultured with LN cells or $CD4^+$ T cells. BLS4-GFP monolayers on chamber slides were cocultured with LN cells or $CD4^+$ T cells for 10 d. Cells were stained with anti–ER-TR7 antibody after fixation and permeabilization, and examined by confocal microscopy. Higher-magnification views show that the ER-TR7 meshwork was frequently positioned in the cell periphery outside the cells (arrowheads). Bars: 100 μm for low- and 30 μm for high-magnification views. (b) BLS4 cells gradually constructed ER-TR7 meshwork during ~1 wk in the coculture system. Cells were stained for ER-TR7 after the indicated number of days of coculturing. Bar, 100 μm. (c) Quantification of ER-TR7 meshwork formation. Total pixels at a certain density window (high: 0–50; medium: 51–100; low: 101–150) of more than five images were calculated and are shown as mean ± SD. We defined high and medium signals as the mature ER-TR7 fibers.

ranges of signal density on the images (Fig. 4 c). During the first few days of coculturing, BLS cells produced a large amount of low-density ER-TR7 antigen, which was detected as intracellular signals or extracellular minute filaments. As the coculture period proceeded, the low-density signals were gradually converted to medium- or high-density concentrated ER-TR7 signals and, thus, we defined these medium- and high-density signals as the mature ER-TR7 fibers. These findings indicate that the ER-TR7 antigen is an ECM component that is secreted from FRCs, accumulated outside the cells, and incorporated into the filamentous network. Importantly, the collaboration of FRCs and lymphocytes accomplishes this work.

TNFα/NF-κB Signaling Participates in the ER-TR7 Meshwork Formation. As the culture supernatant of anti-CD3–stimulated LN cells had a partial but substantial ability to induce meshwork formation by BLS cells (Fig. 5, a and b), soluble factors from lymphocytes appear to be involved. Next, we searched for the factor responsible for inducing meshwork formation and found that TNFα is a candidate with similar activity to the supernatant from activated LN cells; i.e., it showed only partial activity even at high concentrations (up to 100 ng/ml). Other factors, including IL-1, LPS, IFNγ, IL-4, and TGFβ, had no effect (Fig. 5 a and b and not depicted). We also found that TNFα is a growth promoter for BLS cells (unpublished data). Because TNFα activates the NF-κB, chiefly of the RelA (p65)–p50 complex (classical pathway) (33), we introduced IκBαSR, a dominant inhibitor of this signaling pathway (24), into BLS4 cells using a retrovirus vector to examine the involvement of RelA activation in meshwork formation. As expected, stable transfectants were incapable of responding

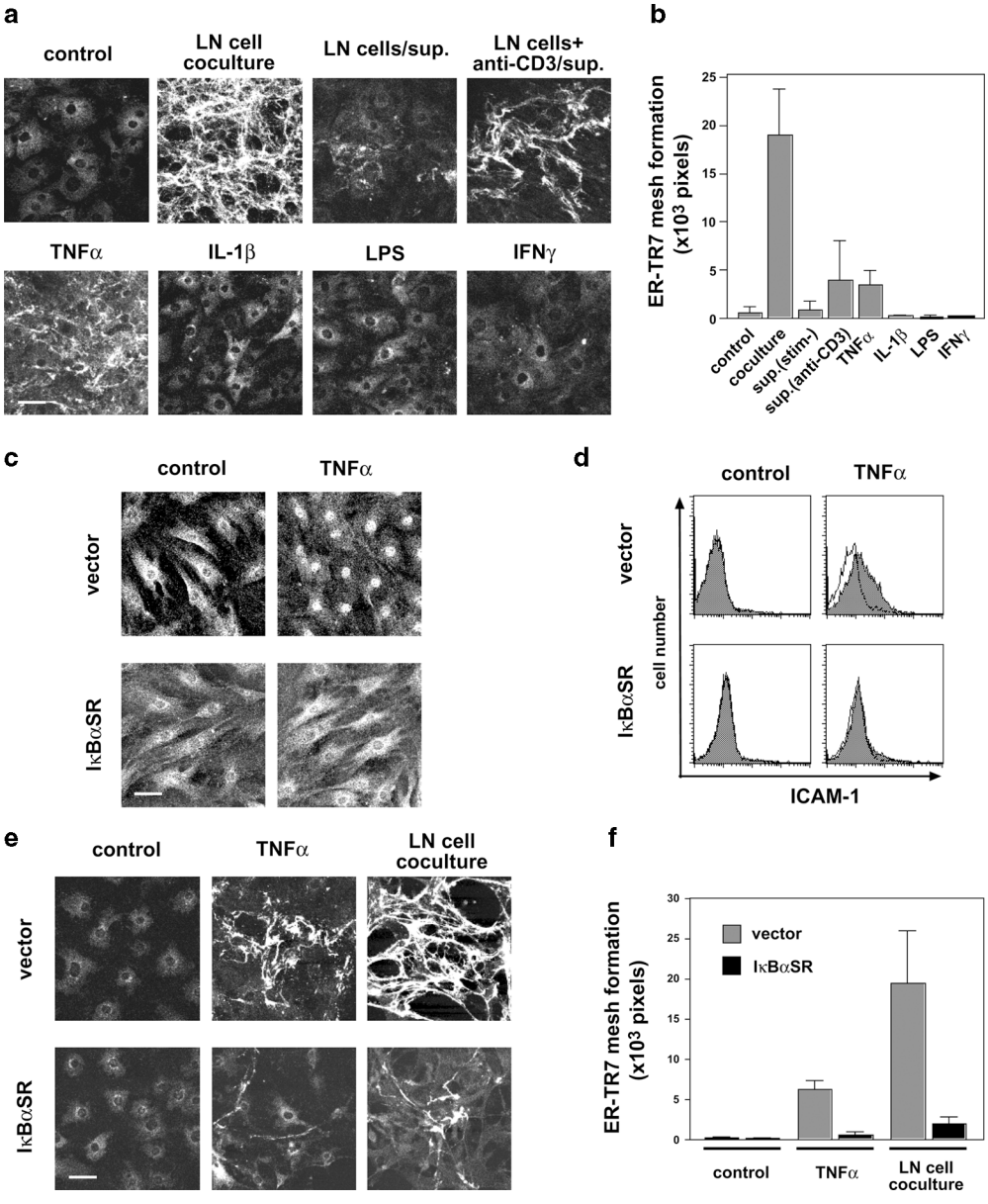

Figure 5. TNFα–NF-κB pathway participates in the ER-TR7 meshwork formation. (a and b) Soluble factors from activated T cells or TNFα partially induce ER-TR7 meshwork in BLS4 cultures. BLS4 cells on chamber slides were cocultured with LN cells or stimulated with LN culture supernatants (in the presence or absence of anti-CD3 antibody) or various cytokines for 10 d and stained with anti–ER-TR7 antibody. Quantification of mature ER-TR7 meshwork (high and medium density) is shown as mean ± SD (b). (c and d) IκBαSR prevents the nuclear translocation of RelA (p65) and expression of ICAM-1 in BLS4 cells. Stable transfectants for control vector or IκBαSR were stimulated with TNFα for 1 h and stained with anti-RelA antibody for confocal microscopic analysis (c) or anti–ICAM-1 antibody for flow cytometry (d). (e and f) IκBαSR inhibits ER-TR7 meshwork formation in BLS4 cultures. Meshwork formation of vector- or IκBαSR-transfectant was examined after 10 d of TNFα stimulation or coculturing with LN cells. Bar, 50 μm. Quantification of mature ER-TR7 meshwork is shown as mean ± SD (f).

to TNFα as assessed by nuclear translocation of RelA protein and the surface expression of a downstream gene product, ICAM-1 (Fig. 5, c and d). We confirmed that this was also the case in IL-1 or LPS stimulation (unpublished data). Strikingly, the IκBαSR-expressing cells were unable to construct the mature ER-TR7 meshwork in response to either TNFα or coculturing with LN cells, although some minute filaments were observed (Fig. 5, e and f). This indicates that RelA activation is indispensable for the meshwork induction. However, as other NF-κB–activating factors such as IL-1 and LPS failed to induce the meshwork, NF-κB activation is not sufficient for this event. Moreover, the fact that TNFα is only able to partially induce ER-TR7 meshwork formation raises the possibility that additional factors might be required for the full construction.

Dual Signaling via TNFR and LTβR Triggers Full Construction of the ER-TR7 Meshwork. LTs, members of TNF family cytokines including soluble homotrimeric LTα and the membrane heterotrimeric form of LTα1β2, are important for lymphoid tissue architecture and organogenesis (19–21). LTα shares its receptors with TNFα (TNFRI and TNFRII) and, thus, the two factors elicit similar effects (20). In contrast, LTα1β2 activates a distinct signaling pathway toward RelB–p52 (p100) (alternative pathway) via LTβR (19–21). Next, we examined the roles of these mediators in the ER-TR7 meshwork formation (Fig. 6, a and b). Stimulation of BLS4 cells with LTα induced only a partial meshwork as expected, similar to the effect of TNFα. Combined stimulation with TNFα and LTα did not enhance the degree of meshwork construction. It is known that several monoclonal antibodies raised against the extracellular part of LTβR mimic receptor engagement and are able to induce downstream signals (34, 35). We used a commercially available polyclonal antibody to the extracellular part of LTβR, which was able to stain the BLS4 cell surface in flow cytometric analysis, trigger the nuclear translocation of RelA (30 min after stimulation) and RelB (4 h), and induce ICAM-1 expression (unpublished data). Addition of this antibody alone to BLS culture did not induce any ER-TR7 meshwork (Fig. 6, a and b). Surprisingly, in the presence of TNFα or LTα, anti-LTβR dramatically enhanced the construction of the meshwork even more efficiently than coculturing with LN cells (Fig. 6, a and b), whereas no effect was induced

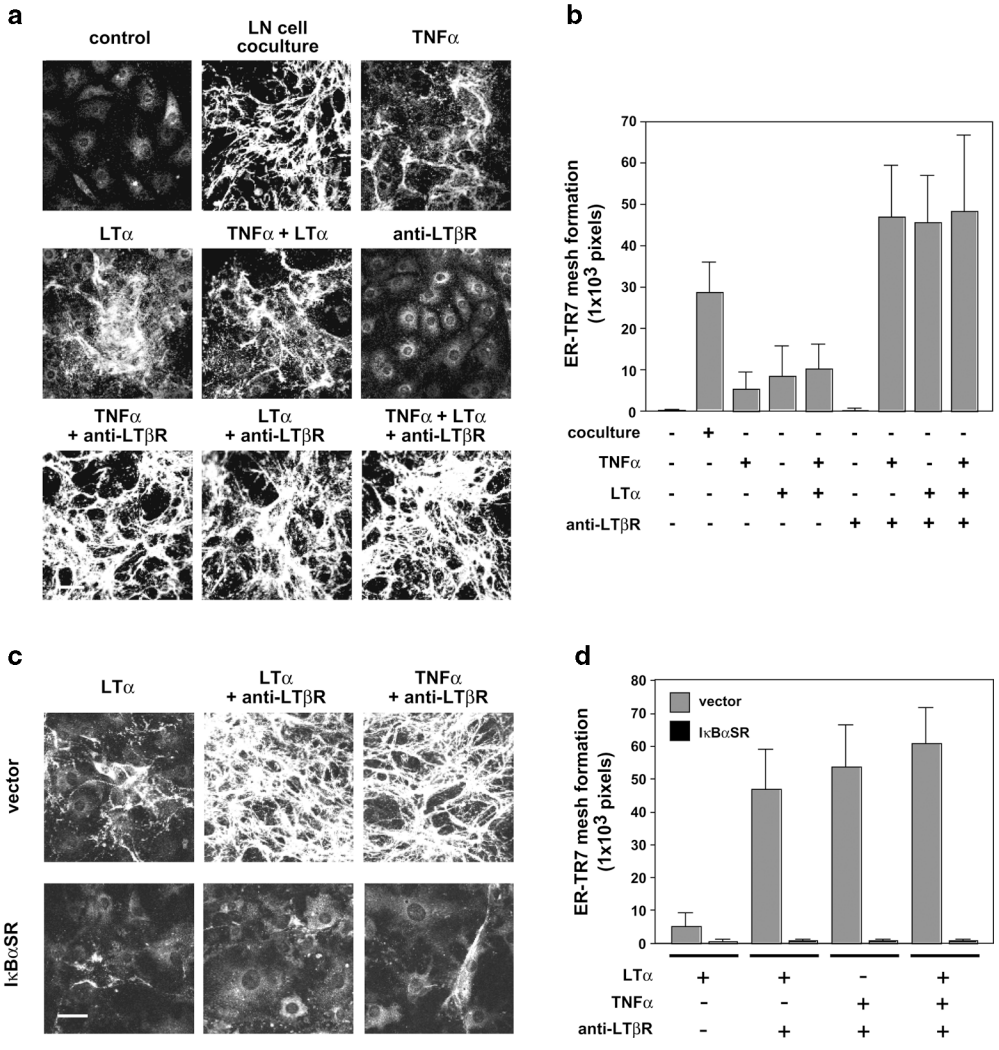

Figure 6. Dual signaling via TNFR and LTβR triggers ER-TR7 meshwork formation. (a) Combined stimulation using agonistic anti-LTβR antibody and TNFα or LTα induces full construction of the ER-TR7 meshwork. BLS4 cells on chamber slides were stimulated with TNFα, LTα, or anti-LTβR antibody, or their combinations, and stained for ER-TR7. Quantification of mature ER-TR7 meshwork is shown as mean ± SD (b). (c and d) IκBaSR inhibits ER-TR7 meshwork formation induced by dual stimulation with TNFR and LTβR. Meshwork formation of transfectants in response to the combinatorial stimulation was examined and quantified. Bar, 50 μm.

by the addition of a control antibody (not depicted). Therefore, simultaneous stimulation through TNFR and LTβR is sufficient for the full construction of the ER-TR7 meshwork by BLS cells. Moreover, combined stimulation with TNFα + anti-LTβR or LTα + anti-LTβR markedly enhanced cell growth and the formation of spike-like cell protrusions (unpublished data). Forced expression of IκBαSR completely inhibited the meshwork formation induced by the combined stimulation (Fig. 6, c and d), demonstrating again that RelA activation is essential. Together, these findings imply that dual signaling via TNFR and LTβR followed by the activation of downstream NF-κB pathways play a powerful role in the meshwork production by BLS cells.

Formation of Three-Dimensional RN by FRCs. Earlier electron microscopic studies showed that FRCs enclose ECM fibers to form a conduit (12). Consistent with these findings, immunohistochemical staining of FRC surface gp38 was localized around the ER-TR7$^+$-RF in tissue sections (Fig. 7 a). This corresponded to the FRC cell body wrapping around the matrix fibers containing ER-TR7, which is well colocalized with other ECM components, such as laminin or fibronectin (Fig. 7, b and c). The colocalization of ER-TR7 with laminin or fibronectin was also observed in the meshwork constructed in vitro (Fig. 7, d and e). Therefore, in response to contact with immune cells, FRCs within the LN probably secrete ER-TR7 antigen along with other ECM components and wrap around them to make the RF.

In our monolayer coculture system, the aforementioned results showed that BLS cells were located in relatively independent positions at the ER-TR7 meshwork (Fig. 4 b). This situation is considerably different from that revealed by the in vivo findings about the RN. It is likely that the flat plastic support kept BLS cells binding to it independently of newly produced ECM, which appears to be a crucial foothold in tissue parenchyma in vivo (16). We consider it possible that under three-dimensional conditions, BLS cells might be able to form an RN-like structure in which cells ensheath the ER-TR7 fibers. To test this, we developed a semi–three-dimensional culture system by using a nylon mesh support coated with laminin. When BLS cells were grown on this mesh, some cells bridged the empty spaces (Fig. 8 a). By adding LN cells to these cultures, BLS growth and the bridging were markedly enhanced, and the ER-TR7 meshwork was formed even in the bridging parts. At higher magnification, we observed that elongated BLS cells enclosed the ER-TR7 fibers at the bridging parts (Fig. 8 a). Optical three-dimensional reconstitution analysis confirmed that BLS4 cells actually enwrapped ER-TR7 fibers at these parts (Fig. 8 b). These experiments suggest that the proper network of FRCs and RF requires close and continuous contact with immune cells in a densely packed three-dimensional space. However, because the RN constructed by BLS cells was apparently immature compared with that constructed in vivo, further steps or factors seem to be required for the completion of the RN in vitro.

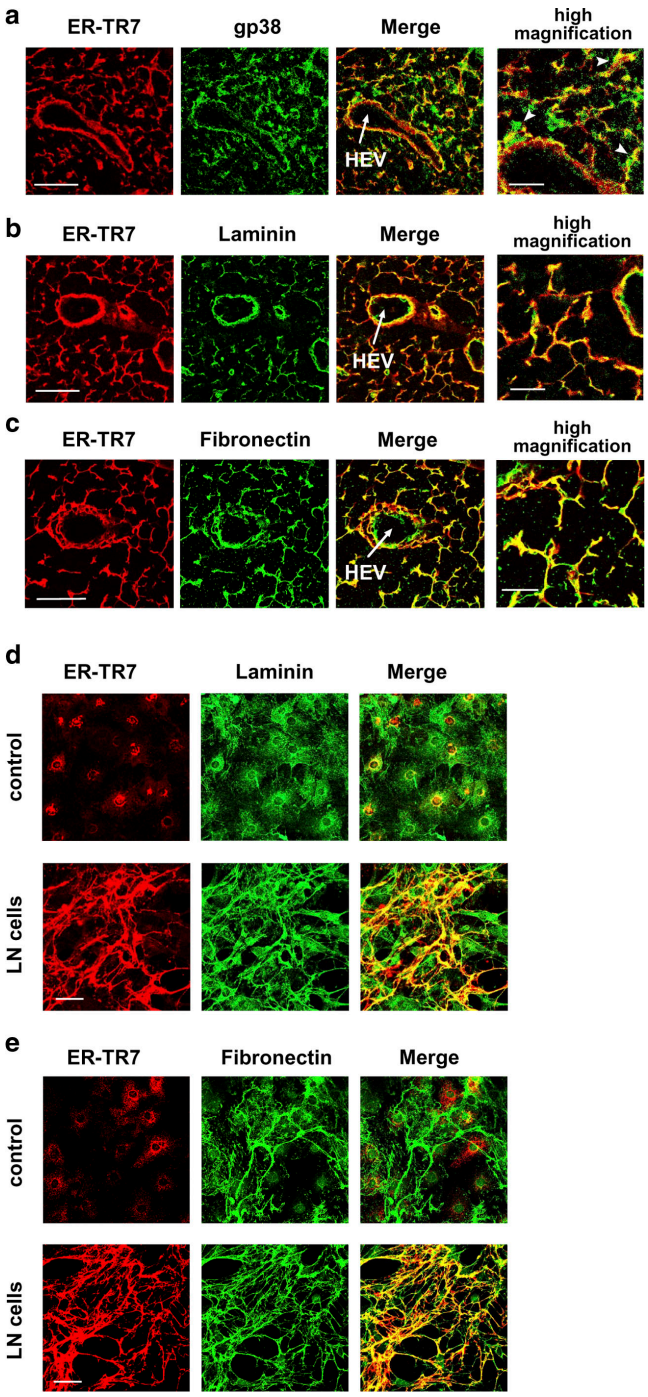

Figure 7. ER-TR7 antigen is secreted as an ECM component. (a) FRC cell body marked by gp38 ensheathes ER-TR7$^+$-RF (arrowheads). (b and c) ER-TR7 is colocalized with laminin (b) and fibronectin (c) in the RN in vivo. LN sections were stained for ER-TR7 and gp38, laminin, or fibronectin. Bars: 50 μm for lower- and 20 μm for higher-magnification views. (d and e) Colocalization of ER-TR7 and laminin (d), or fibronectin (e) in cocultures of BLS4 monolayers with LN cells. Bars, 50 μm.

Discussion

Lymph-hematopoietic cells require specialized supporting milieus where they differentiate, proliferate, survive, or function. The supporting microenvironments or cells are

called stroma or stromal cells, respectively. Stromal functions in primary lymph-hematopoietic tissues, such as bone marrow and thymus, have been well studied because of their crucial importance for maintaining stem cells as well as for cell differentiation (36–41). With regard to secondary lymphoid tissues, researchers have paid a great deal of attention to FDCs residing in B cell follicles and a lot of information about them has been accumulated (2, 5). Several genetic studies have clearly shown that the development of the FDC network depends on B cells that express TNFα and LTs (2). In contrast, the basic features and functions of FRCs have largely remained unclear, despite the fact that they may play an important part in the immune system, as suggested by the fact that they are positioned specifically in the vicinity of lymphocytes and are in physical contact with them. In this work, the establishment of BLS cell lines allowed us to discover some of the unique features of FRCs.

We showed clearly that BLS cells produce an ER-TR7 meshwork via contact with lymphocytes. It is especially worth noting that ER-TR7 antigen proved to be a fibrous ECM component secreted by BLS cells. Although the target that is recognized by ER-TR7 antibody remains to be identified, the findings presented here will be helpful for the identification or further characterization of this antigen in the future. TNFα, LTα, or the culture supernatant of activated lymphocytes partially induced the meshwork, indicating that soluble mediators from lymphocytes play substantial but partial roles in this phenomenon. LTβR ligation does not have the ability to induce the meshwork per se; however, it drastically enhances the induction in collaboration with TNFα or LTα, bringing about the full construction of the meshwork by BLS cells. These results indicate that a dual signal transmitted through TNFR and LTβR is required. Importantly, the ligation of LTβR on BLS cells is thought to be mediated by direct contact with lymphocytes because LTα1β2 is a transmembrane complex on the surface of lymphocytes. Activation of the RelA complex is an essential process for inducing the network formation as well.

The RN in the LN is a three-dimensional structure composed of FRCs and RFs. Dense packing of FRCs and lymphocytes in the space also seems to be crucial for the proper organization of the RN. Under these three-dimensional conditions, FRCs would have no choice but to hold on to the ECM scaffold they had produced, and hence to enwrap the RFs. Our semi–three-dimensional culture system partly succeeded in recapitulating the stringlike reticular structure. However, because the in vivo RN is much more sophisticated than that produced by BLS cells in vitro, there must be additional physiological controls (e.g., the supply of factors from the blood and lymph, directional fluid flow or cell flow, etc.). Together, our findings strongly suggest that lymphocytes and FRCs collaborate to make the LN stromal reticulum through a close interaction depending on the TNF/LT system (Fig. 8 c).

Complete loss of LNs is observed in mice deficient in LTα or LTβR, and most LNs are lost in LTβ-deficient mice (19–21). In contrast, TNFα or TNFRI deficiency results in normal numbers of LNs, although the organization of some tissue architectures is abnormal (19–21). Impor-

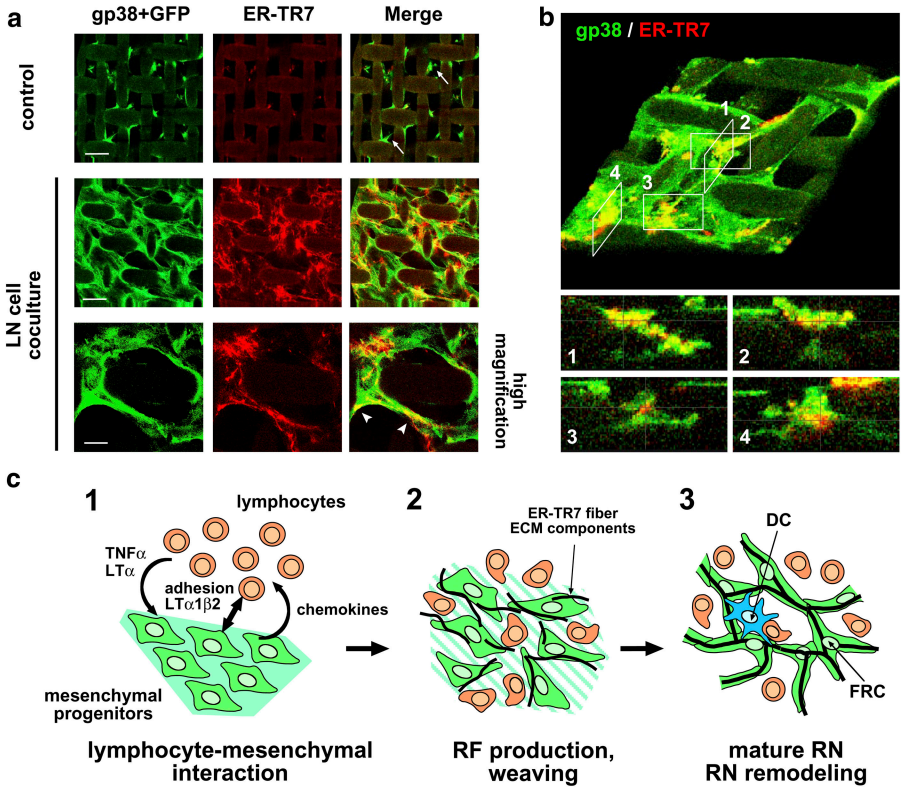

Figure 8. Three-dimensional FRC/RF network construction. (a) Reconstitution of RN-like structure in semi–three-dimensional nylon-mesh culture. BLS4-GFP cells grown on nylon-mesh supports were cocultured with LN cells for 10 d and stained for ER-TR7 and gp38. Note that weak nonspecific background signals were observed on the nylon supports. Bars: top and middle, 50 μm and bottom, 20 μm. (b) BLS4 cells enwrap ER-TR7 fibers. A three-dimensional reconstitution image of the semi–three-dimensional mesh culture stained for gp38 and ER-TR7 was produced from the z-stacks of image data (top, large angled view). Optical sections in the z-plane of appropriate positions (1–4) are shown (bottom). (c) Model of RN formation. (1) Accumulation of lymphocytes induces alteration of mesenchymal progenitors such that they produce chemokines for further lymphocyte attraction and RF components via the secretion of TNFα or LTα (or related cytokines) and likely also via direct contacts mediated by adhesion molecules and LTα1β2. (2) Lymphocytes and differentiated FRCs gradually degrade preexisting matrix, and FRCs weave RF meshwork from the newly produced components. (3) Mature RN forms and antigen presentation occur on the stromal reticulum.

tantly, in utero administration of agonistic anti-LTβR antibody rescues LN development in LTα-deficient mice (34). Accordingly, these observations lead to the conclusion that LTα1β2–LTβR signaling is essential, whereas TNFα, LTα3, and TNFRI are dispensable for LN organogenesis. Mice with combined deficiency for RelA · TNFRI lack all LNs, and TNFRI deficiency rescues embryonic lethality in RelA-deficient mice due to massive hepatocyte apoptosis and, thus, RelA is considered indispensable for LN development (42). Although a small number of LN rudiments develop in RelB-deficient mice, these mice have also been shown to lack all LNs, thus indicating an essential role of RelB in LN development (21). Recently, it was shown that the administration of anti-LTβR antibody did not rescue LN genesis in RORγt-deficient mice, which lack $CD3^{-}CD4^{+}CD45^{+}$ LTi cells, suggesting that the LTα1β2–LTβR axis is necessary but not sufficient for LN genesis (43). Therefore, some other axis that activates RelA provided by LTi cells might be required for the maturation of stromal cells in the LN anlagen.

Splenic white pulp also has an RN structurally and functionally similar to that in the LN (44). Kuprash et al. reported that the ER-TR7^{+} stromal elements in the spleens of various knockout mice, including $TNF^{-/-}$, $LT\beta^{\Delta/\Delta}$, $LT\alpha^{-/-}$, $TNF^{-/-}/LT\alpha^{-/-}$, and TNF/LTΔ3 (lacking TNF, LTα, and LTβ) mice, were progressively reduced and disorganized (45). That work demonstrated that TNF/LT signaling plays an important part in the proper construction of the lymphoid ER-TR7 meshwork in vivo. Substantial but weak ER-TR7 signals were detected even in the spleens of TNF/LTΔ3 mice. This raises the possibility that there are remaining redundant signals for ER-TR7 fiber induction from stromal cells. It is also likely that these remaining ER-TR7^{+} cells are simple parenchymal cells rather than the mature organized lymphoid RN because ER-TR7 antigen is easily detected in the cytoplasm of fibroblasts or the perivascular matrix in nonlymphoid tissues (30).

Collectively, the evidence implies that LN organogenesis and maintenance of the tissue architecture are tightly coupled with stromal specialization in a TNF/LT-dependent fashion. Because the mode of lymphocyte–BLS interaction for constructing an adequate cellular architecture, which is likely to mimic the situation in adult tissues, resembles the inducer–organizer interaction in the anlagen, BLS cells might provide an in vitro model for studying the stromal responses during LN organogenesis.

It remains unclear how each LN subreticular compartment, containing distinct immune cell subsets and thus performing distinct immune reactions, is differentially organized. It may be the case that different FRC subsets construct divergent substructures. For instance, the expression of a chemokine, CCL21 (SLC), a critical factor for T cells and DCs homing into the T zone (46, 47), has been documented to be a specific trait of FRCs only in this area. However, we are as yet unable to detect any CCL21 expression in BLS cells, even if the cells are stimulated with TNFα + LTα + anti-LTβR antibody or cocultured with cell lines (unpublished data). This raises the following three possibilities. First, there is another FRC subset possessing the ability to produce CCL21. Second, established FRC lines have lost this ability. Third, some additional factors are required for BLS cells to express CCL21. It will be an important issue for future studies to determine whether BLS cells are able to produce CCL21 or are actually distinct from the CCL21^{+}-type FRCs, as well as whether there is more than one type of FRC in the LN.

Alternately, the finding that BLS cells have the ability to produce various other chemokines raises the possibility that FRCs could regulate immune cell trafficking and anchoring within the LN. Immune effectors are in a sense "nonstatic" cells and, thus, require firm support and a guide rail for their movement or arrest. Thus, gradients of chemokines or adhesion molecules along FRC surfaces would direct the migration or adhesion of these cells to navigate them to proper sites. Moreover, chemokines produced by FRCs are likely to be transferred to the HEV through RF conduits (13). This should be an effective way to inform circulating lymphocytes about the current LN states. We also detected the expression of several cytokines, including IL-6, IL-7, and IL-15, in BLS cells and, in addition, BLS culture supernatant or coculturing with BLS cells enhances T cell survival (unpublished data), suggesting that FRCs also regulate lymphocyte homeostasis. Thus, the FRC/RN probably serves as the basis of chemokine, cytokine, and adhesion fields for immune interactions or homeostasis. LNs frequently capture metastatic cancer cells from peripheral solid tumors. In those situations, the FRC/RN in turn may provide an opportunity for cancer cells to survive and proliferate via serving as a scaffold or providing growth factors. Recently, malignant cancer cells were shown to express several chemokine receptors and to migrate toward the corresponding ligands (48). Hence, it is urgent to clarify whether FRC-derived factors are involved in cancer metastasis.

The dramatic reorganization of the RN during immune responses shows the great plasticity of FRCs. This flexible nature of the FRC/RN probably takes advantage of the support of the proper types of immune responses. On the other hand, the fact that typical RN structures readily develop in nonlymphoid tissue in cases of chronic inflammation (49) suggests the idea that long-lasting lymphocytes can induce "lymphoid-type" FRCs in extralymphoid tissues as well. This indicates that FRCs are a lineage that can develop from mesenchymal progenitors even in adult tissue environments and change their character drastically upon sensing immune responses. Therefore, in various pathological conditions, FRCs might be a promising target for clinical treatment.

In summary, all the findings obtained in this work strongly support the notion that lymphocytes educate FRCs to weave the RF, to build the specialized network foothold for the immune cells' field of action, and to make the supporting environment that functions as an active component of the immune system.

We are grateful to T. Honjo for allowing us to use a confocal microscope; A.G. Farr for 8.1.1 antibody; M.D. Cooper for anti–BP-3 antibody; H. Wajant for IκBαSR cDNA; T. Kitamura for pMX-

puro plasmid; G.P. Nolan for Phoenix-E cells; and T. Ohfuji for technical assistance.

This work was supported in part by Grants-In-Aid for Science Research on Priority Areas from the Ministry of Education, Culture, Sports, Science and Technology of Japan.

The authors have no conflicting financial interests.

Submitted: 9 February 2004
Accepted: 6 August 2004

References

1. Zinkernagel, R.M., S. Ehl, P. Aichele, S. Oehen, T. Kündig, and H. Hengartner. 1997. Antigen localization regulates immune responses in a dose- and time-dependent fashion: a geographical view of immune reactivity. *Immunol. Revs.* 156: 199–209.
2. Fu, Y.-X., and D.D. Chaplin. 1999. Development and maturation of secondary lymphoid tissues. *Annu. Rev. Immunol.* 17:399–433.
3. Cyster, J.G. 1999. Chemokine and cell migration in secondary lymphoid organs. *Science.* 286:2098–2102.
4. Young, B., and J.H. Heath. 2000. Wheater's Functional Histology. 4th ed. Harcourt Publishers Limited, London.
5. Cyster, J.G., K.M. Ansel, K. Reif, E.H. Ekland, P.L. Hyman, H.L. Tang, S.A. Luther, and V.N. Ngo. 2000. Follicular stromal cells and lymphocyte homing to follicles. *Immunol. Revs.* 176:181–193.
6. von Andrian, U.H., and T.R. Mempel. 2003. Homing and cellular traffic in lymph node. *Nat. Rev. Immunol.* 3:867–878.
7. Banchereau, J., and R.M. Steinman. 1998. Dendritic cells and the control of immunity. *Nature.* 392:245–252.
8. Mcknight, A.J., and S. Gordon. 1998. Membrane molecules as differentiation antigen of murine macrophages. *Adv. Immunol.* 68:271–314.
9. Girard, J.-P., and T.A. Springer. 1995. High endothelial venules (HEVs): specialized endothelium for lymphocyte migration. *Immunol. Today.* 16:449–457.
10. Kraal, G., and R.E. Mebius. 1997. High endothelial venules: lymphocyte traffic control and controlled traffic. *Adv. Immunol.* 65:347–395.
11. Gretz. J.E., E.P. Kaldjian, A.O. Anderson, and S. Shaw. 1996. Sophisticated strategies for information encounter in the lymph node. *J. Immunol.* 157:495–499.
12. Gretz, J.E., A.O. Anderson, and S. Shaw. 1997. Cords, channels, corridors and conduits: critical architectural elements facilitating cell interactions in the lymph node cortex. *Immunol. Revs.* 156:11–24.
13. Gretz, J.E., C.C. Norbury, A.O. Anderson, A.E.I. Proudfoot, and S. Shaw. 2000. Lymph-borne chemokines and other low molecular weight molecules reach high endothelial venules via specialized conduits while a functional barrier limits access to the lymphocyte microenvironments in lymph node cortex. *J. Exp. Med.* 192:1425–1439.
14. Kaldjian, E.P., J.E. Gretz, A.O. Anderson, Y. Shi and S. Shaw. 2001. Spatial and molecular organization of lymph node T cell cortex: a labyrinthine cavity bounded by an epithelium-like monolayer of fibroblastic reticular cells anchored to basement membrane-like extracellular matrix. *Int. Immunol.* 13:1243–1253.
15. Katakai, T., T. Hara, J.-H. Lee, H. Gonda, M. Sugai, and A. Shimizu. 2004. A novel reticular stromal structure in lymph node cortex: an immuno-platform for interactions among dendritic cells, T cells, and B cells. *Int. Immunol.* 16:1133–1142.
16. Cukierman, E., R. Pankov., and K.M. Yamada. 2002. Cell interactions with three-dimensional matrices. *Curr. Opin. Cell Biol.* 14:633–639.
17. Kourilsky, P., and P. Truffa-Bachi. 2001. Cytokine fields and the polarization of the immune response. *Trends. Immunol.* 22:502–509.
18. Vaday, G.G., S. Franitza, H. Schor, I. Hecht, A. Brill, L. Cahalon, R. Hershkoviz, and O. Lider. 2001. Combinatorial signals by inflammatory cytokines and chemokines mediate leukocyte interactions with extracellular matrix. *J. Leukoc. Biol.* 69:885–892.
19. Mebius, R.E. 2003. Organogenesis of lymphoid tissues. *Nat. Rev. Immunol.* 3:292–303.
20. Gommerman, J.L., and J.L. Browning. Lymphotoxin/LIGHT, lymphoid microenvironments and autoimmune disease. *Nat. Rev. Immunol.* 3:642–655.
21. Weih, F., and J. Caamano. 2003. Regulation of secondary lymphoid organ development by the nuclear factor-κB signal transduction pathway. *Immunol. Rev.* 195:91–105.
22. Farr, A.G., M.L. Berry, A. Kim, A.J. Nelson, M.P. Welch, and A. Aruffo. 1992. Characterization and cloning of novel glycoprotein expressed by stromal cells in T-dependent areas of peripheral lymphoid tissues. *J. Exp. Med.* 176:1477–1482.
23. McNagny, K.M., R.P. Bucy, and M.D. Cooper. 1991. Reticular cells in peripheral lymphoid tissues express the phosphatidylinositol-linked BP-3 antigen. *Eur. J. Immunol.* 21:509–515.
24. Kreuz, S., D. Siegmund, P. Scheurich, and H. Wajant. 2001. NF-κB inducers upregulate cFLIP, a cycloheximide-sensitive inhibitor of death receptor signaling, *Mol. Cell. Biol.* 21:3964–3973.
25. Onishi, M., S. Kinoshita, Y. Morikawa, A. Shibuya, J. Phillips, L.L. Lanier, D.M. Gorman, G.P. Nolan, A. Miyajima, and T. Kitamura. 1996. Application of retrovirus-mediated expression cloning. *Exp. Hematol.* 24:324–329.
26. Kinsella, T.M. and G.P. Nolan. 1996. Episomal vectors rapidly and stably produce high-titer recombinant retrovirus. *Hum. Gene Ther.* 7:1405–1413.
27. Inaba, K., M. Inaba, M. Naito, and R.M. Steinman. 1993. Dendritic cell progenitors phagocytose particulates, including bacillus calmette-guerin organisms, and sensitize mice to mycobacterial antigens in vivo. *J. Exp. Med.* 178:479–488.
28. Labeur, M.S., B. Roters, B. Pers, A. Mehling, T.A. Luger, T. Schwarz, and, S. Grabbe. 1999. Generation of tumor immunity by bone marrow-derived dendritic cells correlates with dendritic cell maturation stage. *J. Immunol.* 162:168–175.
29. Katakai, T., T. Hara, M. Sugai, H. Gonda, Y. Nambu, E. Matsuda, Y. Agata, and A. Shimizu. 2002. Chemokine-independent preference for T-helper-1 cells in transendothelial migration. *J. Biol. Chem.* 277:50948–50958.
30. van Vliet, E., M. Melis, J.M. Foidart, and W. van Ewijk. 1986. Reticular fibroblasts in peripheral lymphoid organs identified by a monoclonal antibody. *J. Histo. Cytochem.* 34: 883–890.
31. Schacht, V., M.I. Ramirez, Y.-K. Hong, S. Hirakawa, D. Feng, N. Harvey, M. Williams, A.M. Dvorak, H.F. Dvorak, G. Oliver, and M. Detmar. 2003. T1α/podoplanin deficiency disrupts normal lymphatic vasculature formation and causes lymphedema. *EMBO. J.* 22:3546–3556.
32. Banerji, S., J. Ni, S.-X. Wang, S. Clasper, J. Su, R. Tammi, M. Jones, and D.G. Jackson. 1999. LYVE-1, a new homologue of the CD44 glycoprotein, is a lymph-specific receptor

for hyaluronan. *J. Cell. Biol.* 144:789–801.
33. Baldwin, Jr., A.S. 1996. The NF-κB and IκB proteins: new discoveries and insights. *Annu. Rev. Immunol.* 14:649–681.
34. Rennert, P.D., D. James, F. Mackay, J.L. Browning, and P.S. Hochman. 1998. Lymph node genesis is induced by signaling through the lymphotoxin beta receptor. *Immunity.* 9:71–79.
35. Dejardin, E., N.M. Droin, M. Delhase, E. Haas, Y. Cao, C. Makris, Z.-W. Li, M. Karin, C.F. Ware, and D.R. Green. 2002. The lymphtoxin-β receptor induces different patterns of gene expression via two NF-κB pathways. *Immunity.* 17: 525–535.
36. Petrie, H. 2002. Role of thymic organ structure and stromal composition in steady-state postnatal T-cell production. *Immunol. Revs.* 189:8–19.
37. Anderson, G. and E.J. Jenkinson. 2001. Lymphostromal interactions in thymic development and function. *Nat. Rev. Immunol.* 1:31–40.
38. Dorshkind, K. 1990. Regulation of hemopoiesis by bone marrow stromal cells and their products. *Annu. Rev. Immunol.* 8:111–137.
39. Orkin, S.H. and L.I. Zon. 2002. Hematopoiesis and stem cells: plasticity versus developmental heterogeneity. *Nat. Immunol.* 3:323–328.
40. Heissig, B., K. Hattori, S. Dias, M. Friedrich, B. Ferris, N.R. Hackett, R.G. Crystal, P. Besmer, D. Lyden, M.A.S. Moore, Z. Werb, and S. Rafii. 2002. Recruitment of stem and progenitor cells from the bone marrow niche requires MMP-9 mediated release of Kit-ligand. *Cell.* 109:625–637.
41. Zhang, J., C. Niu, L. Ye, H. Huang, X. He, W.-G. Tong, J. Ross, J. Haug, T. Johnson, J.Q. Feng, et al. 2003. Identification of the haematopoietic stem cell niche and controlof the niche size. *Nature.* 425:836–841.
42. Alcamo, E., N. Hacohen, L.C. Schulte, P.D. Rennert, R.O. Hynes, and D. Baltimore. 2002. Requirement for the NF-κB family member RelA in the development of secondary lymphoid organs. *J. Exp. Med.* 195:233–244.
43. Eberl, G., S. Marmon, M.-J. Sunshine, P.D. Rennert, Y. Choi, and D.R. Littman. 2003. An essential function for the nuclear receptor RORgammat in the generation of fetal lymphoid tissue inducer cells. *Nat. Immunol.* 5:64–73.
44. Nolte, M.A., J.A.M. Beliën, I. Schadee-Eestermans, W. Jansen, W.W.J. Unger, N. van Rooijen, G. Kraal, and R.E. Mebius. 2003. A conduit system distributes chemokines and small blood-borne molecules through the splenic white pulp. *J. Exp. Med.* 198:505–512.
45. Kuprash, D.V., M.B. Alimzhanov, A.V. Tumanov, S.I. Grivennikov, A.N. Shaknov, L.N. Drutskaya, M.W. Marino, R.L. Turetskaya, A.O. Anderson, K. Rajewsky, K. Pfeffer, and S.A. Nedospasov. 2002. Redundancy in tumor necrosis factor (TNF) and lymphotoxin (LT) signaling in vivo: mice with inactivation of the entire TNF/LT locus versus single-knockout mice. *Mol. Cell. Biol.* 22:8626–8634.
46. Gunn, M.D., S. Kyuwa, C. Tam, T. Kakiuchi, A. Matsuzawa, L.T. Williams, and H. Nakano. 1999. Mice lacking expression of secondary lymphoid organ chemokine have defects in lymphocyte homing and dendritic cell localization. *J. Exp. Med.* 189:451–460.
47. Luther, S.A., H.L. Tang, P.L. Hyman, A.G. Farr, and J.G. Cyster. 2000. Coexpression of the chemokines ELC and SLC by T zone stromal cells and deletion of the ELC gene in the plt/plt mouse. *Proc. Natl. Acad. Sci. USA.* 97:12694–12699.
48. Müller, A., B. Homey, H. Soto, N. Ge, D. Catron, M.E. Buchanan, T. McClanahan, E. Murphy, W. Yuan, S.N. Wagner, J.L. Barrera, A. Mohar, E. Verastegui, and A. Zlotnik. 2001. Involvement of chemokine receptors in breast cancer metastasis. *Nature.* 410:50–56.
49. Katakai, T., T. Hara, M. Sugai, H. Gonda, and A. Shimizu. 2003. Th1-biased tertiary lymphoid tissue supported by CXCL13-producing stromal network in the chronic lesions of autoimmune gastritis. *J. Immunol.* 171:4359–4368.